EFFICIENT CONVERSION OF BIOMASS INTO HIGHLY VALUE ADDED CARBON FOR SUPERCAPACITOR ELECTRODE

POOJA A. ZINGARE[a], S.J. DHOBLE[b] AND ABHAY D. DESHMUKH[c1]

[ac]Energy Materials and Devices Laboratory, Department of Physics, R.T.M. Nagpur University, Nagpur, Maharashtra, India

[b]Nanoscience and Nanomaterials Laboratory, Department of Physics, R.T.M. Nagpur University, Nagpur, Maharashtra, India

ABSTRACT

Biomass derived carbons are backbone of emerging carbon based energy storage technology., in the perspective of clean, renewable, cost effective and eco-friendly energy sources. Integration of bio-waste in energy storage devices is a promising approach for efficient waste management. Herein, fallen teak leaves (Tachtona grandis) are used as bio precursor as source of carbon. The as synthesized carbon exhibits superior electrochemical performance with high specific capacitance of 362 F/g at scan rate of 5 mV/s. Also, from GCD studies it exhibits specific capacitance of 263.83 F/g at 0.25 A/g with 99.6% cyclic stability up to 10,000 cycles. In addition, it delivers energy density of 36.64 Wh/kg and power density of 6500 W/kg in three electrode system. Hence, excellent performance of FTLC electrode with notable energy and power densities make it as promising candidate for energy storage application.

KEYWORDS: Biomass, Supercapacitor, Fallen Teak Leaves, Electrochemical Behavior, Cyclic Stability

Development of high performance, renewable and clean energy storage devices is an urge of current era. High demand of portable electronic devices stimulates designing cost effective, flexible and light weight storage devices (Bigdeloo et al., 2021). Batteries does not fulfil demand of rapid charge/discharge and long cycle life hence, advancement of next generation storage technologies is highly felicitous (Kouchachvili et al., 2018). Supercapacitor, attracts vast attention as a promising energy storage device in modernized society due to its exceptional faster power delivery and cyclic stability. Ideally carbon based materials having diverse structural morphologies, high electrical conductivity and greater specific area are explored as supercapacitor electrode materials (Obreja et al., 2010). Additionally, efficient charge storage isotherms provide high reversibility to the carbon electrode. Large number of carbon based materials including graphene, graphite, carbon nanotubes, carbon nanofibers/ cloths and so on were investigated as supercapacitor electrodes (Dubey and Guruviah, 2019). But, the high production cost and tedious synthesis method obstructs widespread commercialization and utilization of these materials. Further along with the selection of carbon precursor execution of eco-friendly approach for synthesis of activated carbon is necessary to adhere the green sustainable chemistry principles (Rashidi et al., 2022).

In the search of readily available, renewable and low cost carbon sources biomass provides promising solution. It is a promising contender for the synthesis of low weight porous carbon for energy storage (Herou et al., 2018). Biomass is abundantly available and highly renewable source of carbon with good ease of harvesting (Vijayakumar et al., 2019). Utilization of biomass resolved issue of waste management and provides value added products. It is the organic waste from plant, animal, industrial by-products and manure. Carbon rich biomass has hierarchical architecture and rich heteroatoms that provides high electrical conductivity and stability to carbon matrix. Biomass composed of long chain polysaccharide compounds in the form of lignin, chitin, cellulose, hemicellulose, protein etc. (Ai et al., 2021). The pyrolysis of biomass converts the chemical composition of carbon into carbon matrix having sufficient phenolic and carboxylic groups (Tan et al., 2021). This carbon backbone has high tensile strength, good corrosion resistance and built with interconnected multiscale porous structure. Biomass derived carbon possess higher specific surface area, thermal and chemical stability and packing density make it promising supercapacitor electrode material (Qiu et al., 2022). The carbonization of biomass yields biochar, activated carbon and less ordered graphitic carbon. Further advanced treatment tends to formation of ordered graphitic layers, graphene oxide, nanotubes and nanofibers. Currently, large number of biomass waste derived carbons have been explored as an electrode material for supercapacitor application showing excellent electrochemical performance (Raza et al., 2018). Recently, areca palm derived biomass derived carbon was synthesized by in-situ chemical activation method. It possesses very high surface area $876 \text{ m}^2/\text{g}$ and delivered high specific

---

[1]Corresponding author

capacitance of 262 F/g at a scan rate of 5 mV/s in Li_2SO_4 electrolyte. The fabricated symmetric cell also shows good energy density of 10.3 Wh/kg and 92% capacitance retention over 5000 charge discharge cycles (Le *et al.*, 2020). Jaychandran *et al.*, synthesized bamboo leaf derived carbon via KOH chemical activation exhibits highly porous morphology. The electrochemical performance was evaluated initially in 1 M Na_2SO_4 shows specific capacitance of 100 F/g at 5 mV/s and then in 0.5 m KOH shows specific capacitance of 80 F/g at same scan rate of 5 mV/s. Further mixing of these two electrolyte i.e. 1 M Na_2SO_4 + 0.5 M KOH significantly enhances the specific capacitance by providing large electrolyte ionic species. The highest specific capacitance was achieved in mix electrolyte was 250 F/g at 5 mV/s from CV curves and 290 F/g at 1 A/g from GCD curves. Also, it shows good cyclic retention of 93% at higher current density 10 A/g up to 10,000 charge discharge cycles (Jayachandran *et al.*, 2021). In an another study Longan leaves derived carbon synthesized using ZnCl2 impregnation. The fabricated coin cell was tested in 1M H_2SO_4 shows specific capacitance of 149 F/g at 1 mV/s and retains 42% of initial capacitance at 10 mV/s (Taer *et al.*, 2021). The durian shell powder derived carbon was prepared by dispersion of powder in H_3PO_4 following hydrothermal method for obtaining hydrochar which later mixed with $(NH_4)_2HPO_4$ and carbonize at high temperature of $800^\circ C$ for obtaining O,N,P doped activated carbon. It delivers specific capacitance of 184 F/g in 1 M H_2SO_4 at 0.5 A/g (Wang *et al.*, 2020). Despite these reported studies, the chemical activation of biomass derived carbon make synthesis methods more tedious also, use of chemicals release toxic gases during activation leading to environment pollution. Also, necessity of inert atmosphere of N_2 or Ar gas overall increases cost of device. Hence, more simplified, scalable and cost effective synthesis method has to be developed.

In this present study, we are using fallen teak leaves as biomass precursor. Teak (*Tectona grandis*) is the tropical plant found in dry forests all over India except J&K. Every year in dry season it shades it's all leaves leading to generation of large scale biomass. These leaves are highly prone to fire and responsible for forest fires. The teak leaves contains 48.51% of carbon and fibrous lignin 22.9% where as 30% of ash contents (Gusmailina *et al.*, 2020). Thus, several efforts are put forward for significant utilization of fallen teak leaves to convert it into useful products. Herein, the teak leaves derived carbon was synthesized using simple carbonization followed by physical activation without use of any external chemicals. It shows great potential to be used as supercapacitor electrode material showing specific capacitance of 362 F/g at 5 mV/s from CV curves

and 263.83 F/g at 0.25A/g from GCD curves in three electrode assembly using 1 M H_2SO_4 electrolyte. Further continuous charge discharge cycles at 9 A/g shows 99.6% initial capacitance retention after 10,000 cycles confirming good cyclic performance of FTLC electrode.

MATERIALS AND METHODS

The dry teak leaves were initially collected from R.T.M. Nagpur university campus in the season of autumn. As collected leaves were then washed with D.I. and dried overnight at 80C followed by crushing using higher power mixer. Further the grinded powder was sieved to obtain fine powder. The fine powder of fallen teak leaves was pyrolyzed at relatively lower temperature of 300°C for 2 hrs. which converts organic matter of fallen teak leaves into carbon. The pyrolyzed carbon elevated at higher temperature of 800°C for 1 hr. in closed charcoal atmosphere for physical activation. It causes microstructural changes in causing and leads to formation of graphitic carbon with more ordered structure. The as obtained graphitic carbon was then etched and washed with 1 M HCl to remove remnant traces of inorganic impurities from sample. After drying overnight, the final product was named as FTLC in further discussion.

For preparation of working electrode stainless steel mesh (SS) was used as substrate. The slurry was prepared using FTLC, carbon black and PVDF binder in ration 8:1:1 mixed with few drops of NMP to form uniform slurry. The slurry was then coated over sample and dried in vacuum overnight at 80°C. Further all the electrochemical measurements were done using FTLC electrode.

RESULTS AND DISCUSSION

Physical Characterizations

Schematic of synthesis of FTLC is as shown in Fig.1a. Briefly FTLC was prepared by low temperature pre carbonization followed by physical activation at 800°C for obtaining activated carbon. The structural and morphological studies of carbon are essential to define their utility in further energy storage application. The FTLC carbon was characterized using XRD for determining structural analysis, FTIR analysis for functional group analysis and SEM for morphological analysis. The XRD pattern of FTLC was recorded between 2θ degrees 10 ˚ -70˚ (Fig. 1b). It consists of two broad peaks corresponding to amorphous nature of carbon. The most prominent peak at 23.4˚ is resultant of reflection from (002) plane and another less intense peak at 42.8˚ is corresponds to reflection from (100) plane confirms graphitic phase of carbon (Wang *et al.*, 2012).
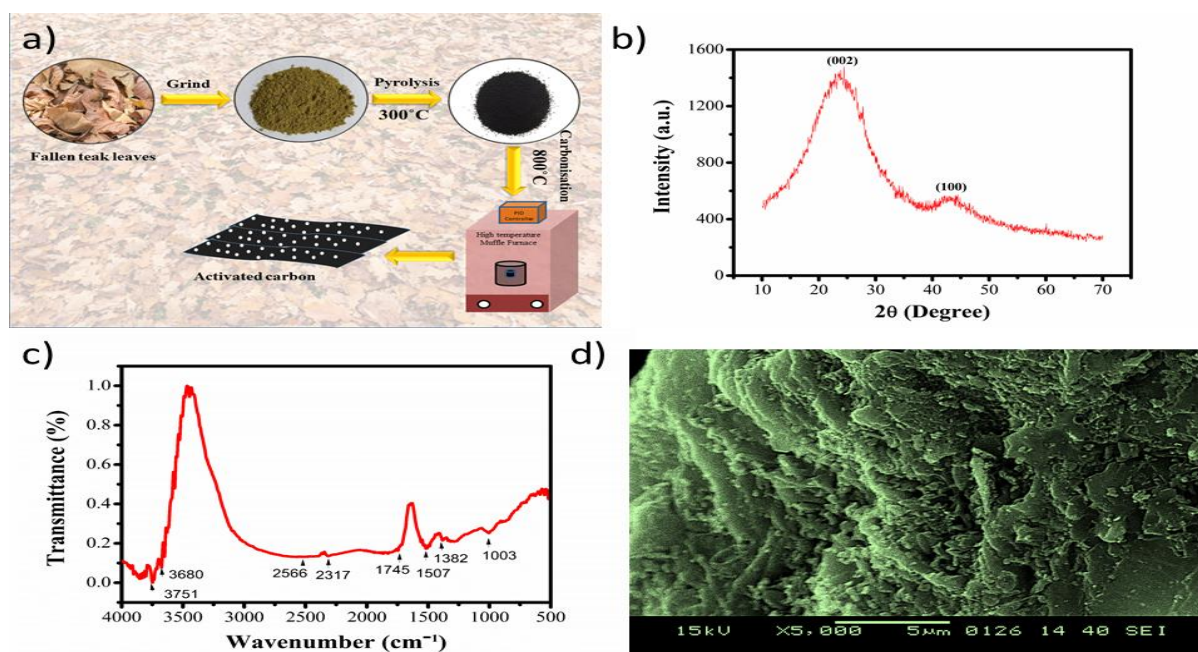
Figure 1: a) Schematic of synthesis of fallen teak leaves derived carbon (FTLC). b) XRD spectra of FTLC revealing amorphous nature of carbon. c) FTIR analysis of FTLC in wavenumber range 4000-500 cm^{-1} depicts numerous functional groups. d) Morphological analysis of FTLC with SEM

The interlayer spacing calculated using Scherer formula corresponding to peak found to be d$_{200}$ = 0.38 nm and the calculated crystallized size was 16.9 nm. These small values of interlayer spacing provide good ion reservoir for ion transportation. The FTIR spectra recorded in wavenumber region 500-4000 cm^{-1} (Fig. 1c) shows several peaks in the region between 3000-4000 cm^{-1} confirms presence of –OH stretching vibrations. Meanwhile peak at 2566 cm^{-1} shows C=H stretching vibrations. O=C=O strong bond appears at wavenumber 2317 cm^{-1} and peaks around 1800 cm^{-1} to 1700 cm^{-1} shows C=O stretching vibrations. The C-H bending of aldehyde group appears at 1382 cm^{-1} and C=C bending at 1003 cm^{-1} (Zhu *et al.*, 2018). The morphological analysis was studied using SEM analysis as shown in Fig.1d. It shows uniformly distributed carbon matrix bearing pores. It provides good surface area for ion accumulation and pores can efficiently works as charge transfer paths (Minakshi Gohain *et al.*, 2020). This ultimately supports good electrochemical behavior of electrode.

Electrochemical Measurements

The supercapacitive parameters were calculated from cyclic voltammetry (CV), galvanic charge discharge (GCD) and electrochemical impedance spectroscopy (EIS) in 1 M H$_2$SO$_4$ electrolyte against Ag/AgCl as reference electrode and platinum plate as counter electrode. CV voltagram was obtained at various scan rates from 5 mV/s to 100 mV/s within constant potential window of -0.2 V -0.8 V (Fig.2a). CV curves measures current response of electrode material versus potential. It

shows quasi rectangular shape as consequence of surface controlled reversible absorption desorption charge storage isotherm. Increasing scan rate area under curve increases as large number of electrolyte ions accumulated at the electrode surface while very small number of ions actually contributes to charge storage (Li *et al.*, 2019). Importantly, the shape of CV curves remains same at higher scan rates confirming excellent rate capability and reversibility of FTLC electrode. Further the specific capacitance was calculated from CV curves using relation (Yan *et al.*, 2010),

$$C_s = \frac{\int I\,dv}{m * v * V} \qquad (1)$$

Where, $\int I\,dv$ is the integrated area under curve, m is the mass of electrode, v is scan rate and V is the potential window.

The highest obtained value of C$_s$ is 362 F/g at 5 mV/s and remain high as 308.5 F/g at 100 mV/s showing high capacitance retention of 85% and the variation of specific capacitance at various scan rates was illustrated in Fig.2c. Further, power law I= a v^b determines charge transfer kinetics of the electrode, where, I is the peak current, v is scan rates and a and b are constant parameters (Fig. 2b). b value depicts whether the charge storage is dominated by surface controlled reaction or diffusion controlled reactions. b = 0.5 reveals charge storage is attributed to intercalation of ions whereas, b =1 confirms adsorption and desorption of ions at the electrode electrolyte interface responsible for charge storage (Deepa *et al.*, 2022). For FTLC electrode value of

b was found to be 1.04 demonstrates charge storage mechanics follows purely EDLC behavior.

The galvanic charge discharge (GCD) study determines the capacitive behavior of FTLC electrode. The GCD curves were analyzed at various scan rates from 0.25 A/g to 13 A/g in 1 M H_2SO_4. Fig.2d shows typical symmetric triangular curves as characteristic of double layer capacitance. The small value of IR drop implies low internal resistance and high power delivering capacity of electrode. The specific capacitance at various current densities calculated from GCD curves using relation (Maher *et al.*, 2021),

$$C_s = \frac{I\,\Delta t}{m\,\Delta V} \qquad (2)$$

Where, I is the applied current, Δt is the discharge time, ΔV is the potential difference and m is the mass loading of the electrode. The highest specific capacitance for FTLC was found to be 263.83 F/g at 0.25A/g whereas, 237.2 F/g, 221.8 F/g, 202.4 F/g, 192.6 F/g, 187.6 F/g, 180.7 F/g and 174.2 F/g at current densities of 0.5 A/g, 1 A/g, 3 A/g, 5 A/g, 7 A/g, 9 A/g and 13 A/g respectively. The high specific capacitance of FTLC attributed to the interconnected pore distribution. It fascinates excellent charge and electrolyte ion transport through the carbon matrix and significantly leads to enhancement of specific capacitance. Hence, manifests good capacitance retention of 66% at higher current density 13 A/g. The capacitance retention at higher current densities due to nanostructured carbon morphology which allows better segregation of electrolyte ions even at higher current densities. More importantly, energy and power density is the measure of practical utility of electrode material and are calculated using relations (Qui *et al.*, 2022),

$$E = \frac{CV^2}{2\times 3.6} \qquad \text{Wh/kg} \qquad (3)$$

$$P = \frac{E\times 3600}{t} \qquad \text{W/kg} \qquad (4)$$

Interestingly, the prepared FTLC delivers highest energy density 36.64 Wh/kg at 125 W/kg power density and highest power density 6500 W/kg at energy density 24 Wh/kg. The Ragone chart of energy and power density shows outstanding energy and power response of FTLC electrode (Fig.2e). The electrochemical performance of FTLC in three electrode system was consolidated in Table 1. Results reveals high potential of FTLC electrode in high energy and power utility applications. The cycle life of an electrode is an another important aspect determining practical suitability of electrode. The FTLC shows highest stability of 99.6 % in three electrode system up to 10,000 continuous charge discharge cycles at higher current density of 9 A/g with 98% coulombic efficiency (Fig2f). The excellent cycle life with ability to store high energy and fast power delivery make FTLC a promising supercapacitor electrode.
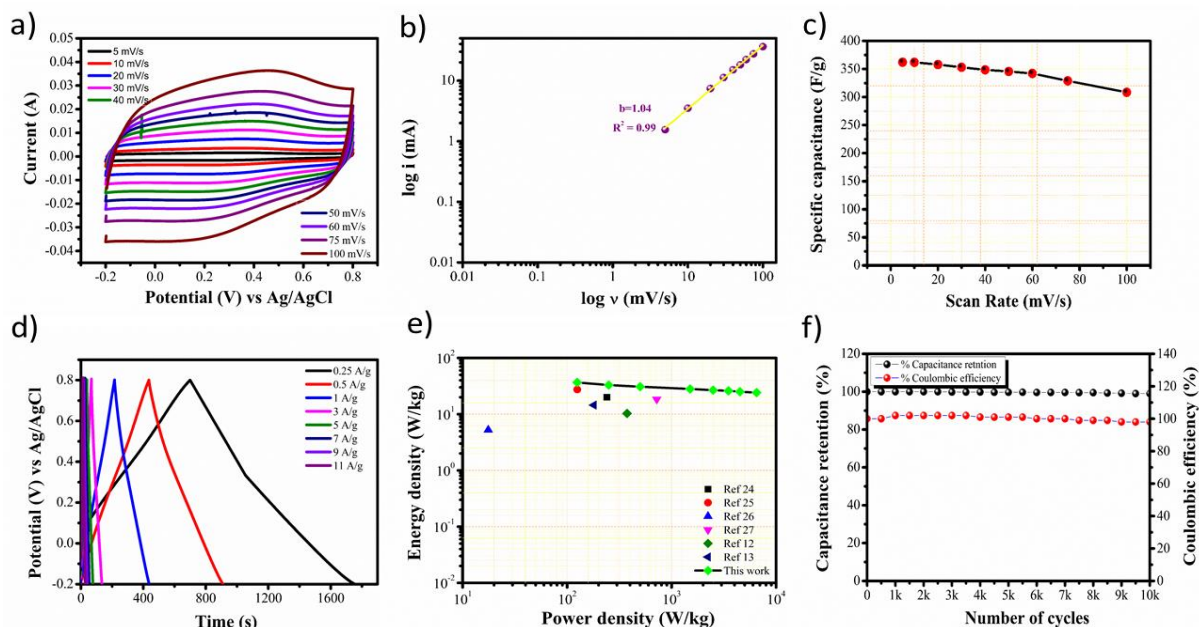

Figure 2: a) Cyclic voltammetry curves of FTLC at various scan rates from 5 mV/s -100 mV/s in 1 M H_2SO_4. b) Power law determining surface and diffusion controlled contribution of FTLC. c) Variation of specific capacitance as function of scan rates. d) Galvanic charge discharge curves of FTLC at different current densities from 0.25 A/g – 13 A/g. e) Ragone plot of energy and power density of FTLC compared with other recently reported literature. f) Capacitance retention and Coulombic efficiency of TLC auto 10,000 charge discharge cycles

Table 1: Electrochemical performance of FTLC in three electrode system in 1 M H_2SO_4

Scan rate (mV/s)	Specific Capacitance (F/g)	Current density (A/g)	Specific Capacitance (F/g)	Energy density (Wh/kg)	Power density (W/kg)
5	362.14	0.25	263.83	36.64	125
10	361.9	0.5	237.225	32.94	250
20	357.95	1	221.4	30.8	500
30	353.06	3	202.44	28.11	1500
40	348.57	5	192.6	26.75	2500
50	345.71	7	187.6	26.05	3500
60	342.02	9	180.6	25.1	4500
75	328.91	13	174.2	24.19	6500
100	308.5				

Table 2: Comparative electrochemical performance of biomass derived carbon with FTLC in three electrode configuration

Biomass precursor	Electrolyte	Specific capacitance (F/g)	Energy density (Wh/kg)	Power density (W/kg)	Cyclic retention	References
Rice husk	6M KOH	197.4 at 2 mV/s	20	240	99 % up to 1000 cycles	(Le Van and Luong Thi, 2014)
Fish scales	1M H_2SO_4	195 F/g at 0.25 A/g	27.4	125	100% up to 10,000 cycles	(Zingare et al., 2022)
Orange peel	1M KOH	144 at 2 mV/s	5.27	17.59	72% up to 5000 cycles	(Ajay et al., 2021)
Corn silk	1M $TEABF_4$/PC	86.4 at 1 A/g	18.4	720.8	84% up to 2500 cycles	(Mitravinda et al., 2018)
Areca Palm	1 M Li_2SO_4	262 F/g at 5 mV/s	10.3	375	92% up to 5000 cycles.	(Le et al., 2020)
Bamboo leaf	1M Na_2SO_4+0.5 M KOH	250 F/g at 5 mv/s	14.5	180	93% up to 1000 cycles	(Jayachandran et al., 2021)
Fallen Teak leaves	1M H_2SO_4	362 F/g at 5 mV/s	36.14	6500	99.6% up to 10,000 cycles	This work

Resistive parameters of electrode are necessary for determining the internal resistance. It was evaluated from electrochemical impedance spectroscopy (EDLC). Fig.3a shows the Nyquist plot of FTLC measured in the frequency range 0.01 Hz to 100 kHz with an open circuit potential 0.365. It consists of three regions, i) a lower frequency region consists of line inclined parallel to imaginary impedance axis indicating capacitive behavior of electrode, ii) a middle frequency region shows the effect of electrode thickness and porosity on the diffusion of electrolyte ions into the electrode, iii) a high frequency region consists of semicircle and electrode behave as pure resistor in this region and it is called as blocking region of electrode (Sundriyal et al., 2021). It is the combination of equivalent series resistance R_s (resistance between substrate and working electrode, electrode electrolyte interface well as internal resistance of the electrode) and charge transfer resistance R_{ct} (solution resistance to the transfer ions into electrode surface). Lower values of resistances shows enhanced charge transfer kinetics of electrode and hence specific capacitance. The values of R_s and R_{ct} obtained from Nyquist plots are 0.739 Ω and 1.744 Ω further the fit and simulated Nyquist plot using Randle's circuit shows R_s and R_{ct} values of 0.698 Ω and 0.958 Ω respectively. The well matched obtained and simulated values of equivalent series resistance and charge transfer resistance confirms high performance of electrode. The C_{dl} from fitted circuit represents double layer capacitance, Z_w is the Warburg impedance and Z_{CPE} is the constant phase element indicating deviation from ideal capacitive behavior. Constant phase element defined as $Z_{CPE} = [Y_0(j\omega)^n]^{-1}$ and it is independent of frequency. Value of n lies between -1 to 1 and depicts capacitive, conductive or resistive behavior of an

electrode. For n = 1 CPE behave as pure capacitor, with n = -1 it act as pure inductor and resistor for n = 0 (Scisco *et al.*, 2021). The value of n for FTLC was 0.99 demonstrating pure capacitive behavior. Moreover, Bode plots as shown in Fig.3b shows bode phase angle at -83⁰ revealing capacitive behavior of electrode. The complex capacitance illustrated as,

$$C(\omega) = C'(\omega) + j\, C''(\omega) \quad (5)$$

where, $C'(\omega)$ is the real part of the capacitance and $C''(\omega)$ is the imaginary part of capacitance and given as,

$$C'(\omega) = \frac{-Z''(\omega)}{\omega\, |Z(\omega)|^2} \quad (6)$$

$$C''(\omega) = \frac{Z'(\omega)}{\omega\, |Z(\omega)|^2} \quad (7)$$

Here, Z' and Z" are real and imaginary impedance. The relaxation time of an electrode further obtained from frequency corresponding to half of the maximum value of real part of capacitance or frequency corresponding to the peak of imaginary capacitance graph which attributed to the maximum energy dissipated from system (Jain and Tripathi, 2015). The relaxation time from C' plot was found to be 4.1 s (Fig. 3c). Additionally, complex power $S(\omega) = P(\omega) + j\, Q(\omega)$ can also demonstrates relaxation time from P/S and Q/S plots given as (Mehare *et al.*, 2020),

$$P(\omega) = \omega\, C''(\omega)|V^2_{rms}| \quad (8)$$

$$Q(\omega) = -\omega\, C'(\omega)|V^2_{rms}| \quad (9)$$

where, $V_{rms} = \Delta V_{max}/\sqrt{2}$ and ΔV_{max} is the maximum potential.

The plots of P/S and Q/S have exactly opposite behavior (Fig. 3d). The frequency belongs to intersection of complex power plots gives relaxation time. Low frequency corresponds to zero power (P = 0) dissipated to the system corresponding to pure capacitive behavior and higher frequency region power dissipated is 100% depicts pure resistive behavior of system (Zingare *et al.*, 2022). From complex power plot relaxation time of an electrode was found to be 3.5 s. The small relaxation time from both graphs confirms FTLC electrode is capable for providing sudden high power burst make it as promising electrode in high power delivering application. Hence, with ability to provide high specific capacitance, long cycle life, high rate capability and very small value of internal resistance make FTLC as a promising supercapacitor electrode.
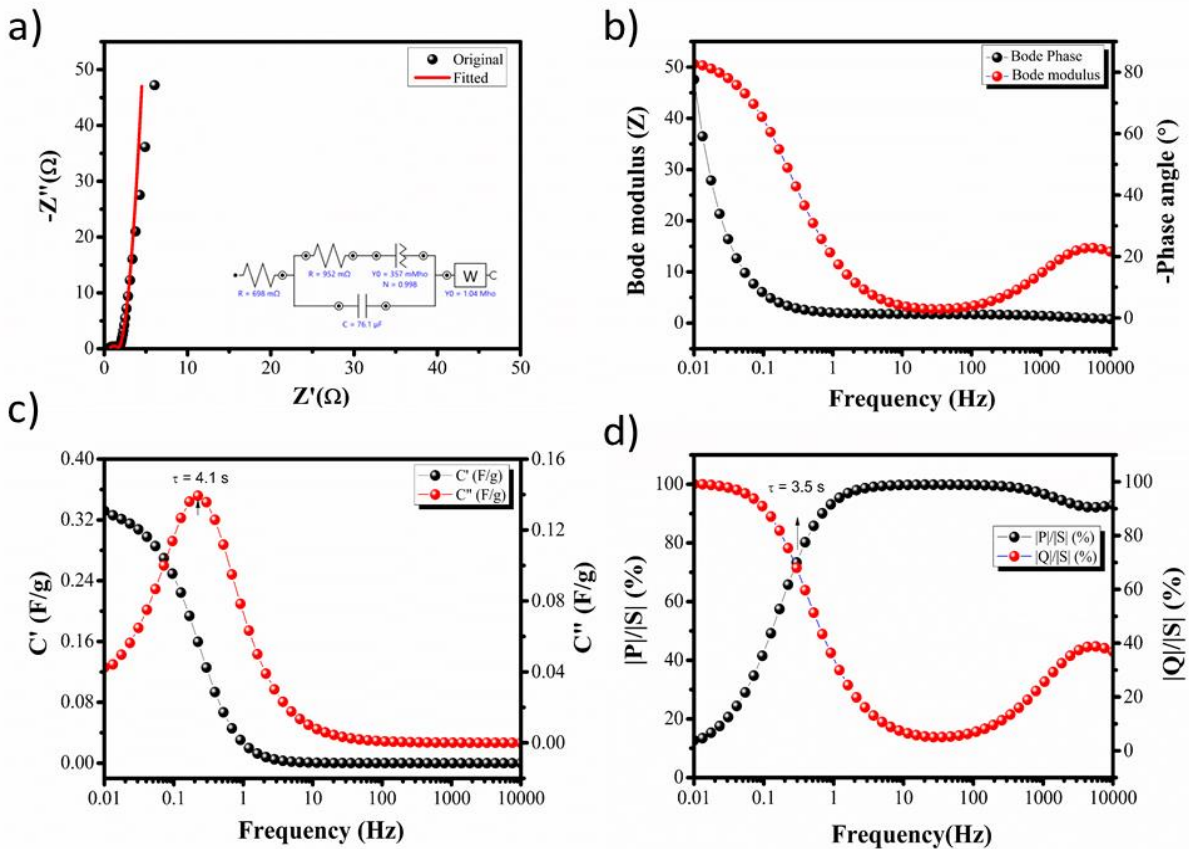

Figure 3: a) Nyquist plot of FTLC in frequency range 0.1 Hz to 10000 Hz with equivalent fitted circuit in the inset. b) Bode modulus and bode phase plots of FTLC. c) Real and imaginary capacitance as function of frequency determining relaxation time of electrode. d) Complex power plots of FTLC as function of frequency

CONCLUSION

In summary, biomass derived carbon was efficiently synthesized using waste fallen teak leaves via facile, green and sustainable chemical free approach. The prepared FTLC shows abundant oxygen functional groups which provides electroactive sites and increases wettability of carbon. The FTLC carbon shows highest specific capacitance of 362 F/g at scan rate of 5 mv/s and 263.83 F/g at a current density of 0.25 A/g in three electrode system. The FTLC carbon also delivers highest energy density of 36.64 Wh/kg and power density of 6500 W//kg. Further, it proves its excellency to be used as supercapacitor electrode material by showing 99.6% capacitance retention up to 10,000 charge discharge cycles. Interestingly, FTLC electrode with high specific capacitance, good energy and power density and superior cycle life performance proves as promising electrode material for high energy and power supercapacitor applications.

ABBREVIATIONS

FTLC – Fallen Teak Leaves derived carbon, , PVDF- Polyvinylidene fluoride; CV – Cyclic Voltammetry, EDLC - Electrochemical Double Layer capacitors, XRD – X-ray Powder Diffraction, FTIR- Fourier Transform Infrared, SEM-Scanning Electron Microscopy

ACKNOWLEDGEMENTS

CONFLICTS OF INTEREST

The authors declare that they have no known conflict of interests.

REFERENCES

Ai J., Yang S., Sun Y., Liu M., Zhang L., Zhao D., Wang J., Yang C., Wang X. and Cao B., 2021. "Corncob cellulose-derived hierarchical porous carbon for high performance supercapacitors". J. Power Sources, **484**: 229221, doi: 10.1016/j.jpowsour.2020.229221.

Ajay K.M., Dinesh M.N., Byatarayappa G., Radhika M.G., Kathyayini N. and Vijeth H., 2021. "Electrochemical investigations on low cost KOH activated carbon derived from orange-peel and polyaniline for hybrid supercapacitors". Inorg. Chem. Commun., **127**, doi: 10.1016/j.inoche.2021.108523.

Bigdeloo M., Kowsari E., Ehsani A., Chinnappan A., Ramakrishna S. and AliAkbari R., 2021. "Review on innovative sustainable nanomaterials to enhance the performance of supercapacitors". J. Energy Storage, **37**: 102474, doi: 10.1016/j.est.2021.102474.

Deepa B. Bailmare, Mrunali D. Wagh, Narkhede N., Sharma R.K. and Deshmukh A.D., 2022. "Nitrogen optimized highly stable carbon for increasing the efficiency of supercapacitors". Int. J. Energy Res., doi: https://doi.org/10.1002/er.8285.

Dubey R. and Guruviah V., 2019. "Review of carbon-based electrode materials for supercapacitor energy storage," Ionics (Kiel)., **25**(4): 1419–1445, doi: 10.1007/s11581-019-02874-0.

Gusmailina, Komarayati S. and Wibisono H.S., 2020. "Potential uses of teak leaf litter for liquid smoke and of other utilizations: A review". IOP Conf. Ser. Mater. Sci. Eng., **935**(1), doi: 10.1088/1757-899X/935/1/012015.

Herou S., Schlee P., Jorge A.B. and Titirici M., 2018. "Biomass-derived electrodes for flexible supercapacitors," Curr. Opin. Green Sustain. Chem., **9**: 18–24, doi: 10.1016/j.cogsc.2017.10.005.

Jayachandran M., Kishore Babu S., Maiyalagan T., Rajadurai N. and Vijayakumar T., 2021. "Activated carbon derived from bamboo-leaf with effect of various aqueous electrolytes as electrode material for supercapacitor applications". Mater. Lett., **301**: 130335, doi: 10.1016/j.matlet.2021.130335.

Jain A. and Tripathi S.K., 2015. "Nano-porous activated carbon from sugarcane waste for supercapacitor application". J. Energy Storage, **4**: 121–127, doi: 10.1016/j.est.2015.09.010.

Kouchachvili L., Yaïci W. and Entchev E., 2018. "Hybrid battery/supercapacitor energy storage system for the electric vehicles". J. Power Sources, **374**: 237–248, doi: 10.1016/j.jpowsour.2017.11.040.

Le P.A., Nguyen V.T., Sahoo S.K., Tseng T.Y. and Wei K.H., 2020. "Porous carbon materials derived from areca palm leaves for high performance symmetrical solid-state supercapacitors". J.

Mater. Sci., **55**(24): 10751–10764, doi: 10.1007/s10853-020-04693-5.

Le Van K. and Luong Thi T.T., 2014. "Activated carbon derived from rice husk by NaOH activation and its application in supercapacitor". Prog. Nat. Sci. Mater. Int., **24**(3): 191–198, doi: 10.1016/j.pnsc.2014.05.012.

Li J., Gao Y., Han K., Qi J., Li M. and Teng Z., 2019. "High performance hierarchical porous carbon derived from distinctive plant tissue for supercapacitor". Sci. Rep., **9**(1): 17270.

Maher M., Hassan S., Shoueir K., Yousif B. and Abo-Elsoud M.E.A., 2021. "Activated carbon electrode with promising specific capacitance based on potassium bromide redox additive electrolyte for supercapacitor application". J. Mater. Res. Technol., **11**: 1232–1244, doi: 10.1016/j.jmrt.2021.01.080.

Mehare M.D., Deshmukh A.D. and Dhoble S.J., 2020. "Preparation of porous agro-waste-derived carbon from onion peel for supercapacitor application". J. Mater. Sci., **55**(10): 4213–4224, doi: 10.1007/s10853-019-04236-7.

Minakshi Gohain D.D., Khairujjaman Laskar, Hridoyjit Phukon, Bora U. and Kalita D., 2020. "Towards sustainable biodiesel and chemical production: Multifunctional use of heterogeneous catalyst from littered Tectona grandis leaves". Waste Manag., **102**: 212–221.

Mitravinda T., Nanaji K., Anandan S., Jyothirmayi A., Chakravadhanula V.S.K., Sharma C.S. and Rao T.N., 2018. "Facile Synthesis of Corn Silk Derived Nanoporous Carbon for an Improved Supercapacitor Performance". J. Electrochem. Soc., **165**(14).

Obreja V.V.N., Dinescu A. and Obreja A.C., 2010. "Activated carbon based electrodes in commercial supercapacitors and their performance". Int. Rev. Electr. Eng., **5**(1): 272–281.

Qiu G., Miao Z., Guo Y., Xu J., Jia W., Zhang Y., Guo F. and Wu J., 2022. "Bamboo-based hierarchical porous carbon for high-performance supercapacitors: the role of different components". Colloids Surfaces A Physicochem. Eng. Asp., **650**: 129575, doi: 10.1016/j.colsurfa.2022.129575.

Rashidi N.A., Chai Y.H., Ismail I.S., Othman M.F.H. and Yusup S., 2022. "Biomass as activated carbon precursor and potential in supercapacitor applications". Biomass Convers. Biorefinery, 0123456789, doi: 10.1007/s13399-022-02351-1.

Raza W., Ali F., Raza N., Luo Y., Kim K.-H., Yang J., Kumar S., Mehmood A. and Kwon E.E., 2018. "Recent advancements in supercapacitor technology," Nano Energy, **52**: 441–473, doi: 10.1016/j.nanoen.2018.08.013.

Scisco G.P., Orazem M.E., Ziegler K.J. and Jones K.S., 2021. "On the rate capability of supercapacitors characterized by a constant-phase element". J. Power Sources, **516**: 230700, doi: 10.1016/j.jpowsour.2021.230700.

Sundriyal S., Shrivastav V., Kaur A., Mansi, Deep A. and Dhakate S.R., 2021. "Surface and diffusion charge contribution study of neem leaves derived porous carbon electrode for supercapacitor applications using acidic, basic, and neutral electrolytes". J. Energy Storage, **41**: 103000, doi: 10.1016/j.est.2021.103000.

Tan Z., Yang J., Liang Y., Zheng M., Hu H., Dong H., Liu Y. and Xiao Y., 2021. "The changing structure by component: Biomass-based porous carbon for high-performance supercapacitors". J. Colloid Interface Sci., **585**: 778–786, doi: 10.1016/j.jcis.2020.10.058.

Taer E., Tampubolon D.K.H., Apriwandi, Farma R., Setiadi R.N. and Taslim R., 2021. "Longan leaves biomass-derived renewable activated carbon materials for electrochemical energy storage," J. Phys. Conf. Ser., **2049**(1), doi: 10.1088/1742-6596/2049/1/012009.

Vijayakumar M., Bharathi Sankar A., Sri Rohita D., Rao T.N. and Karthik M., 2019. "Conversion of Biomass Waste into High Performance Supercapacitor Electrodes for Real-Time Supercapacitor Applications," ACS Sustain. Chem. Eng., **7**(20): 17175–17185, doi: 10.1021/acssuschemeng.9b03568.

Wang K., Zhang Z., Sun Q., Wang P. and Li Y., 2020. "Durian shell-derived N, O, P-doped activated porous carbon materials and their electrochemical performance in supercapacitor". J. Mater. Sci., **55**(23): 10142–10154, doi: 10.1007/s10853-020-04740-1.

Wang R., Wang P., Yan X., Lang J., Peng C. and Xue Q., 2012. "Promising porous carbon derived from celtuce leaves with outstanding supercapacitance and CO2 capture performance". ACS Appl.

Mater. Interfaces, **4**(11): 5800–5806, doi: 10.1021/am302077c.

Yan J., Wei T., Shao B., Fan Z., Qian W., Zhang M. and Wei F., 2010. "Preparation of a graphene nanosheet/polyaniline composite with high specific capacitance". Carbon N.Y., **48**(2): 487–493, doi: 10.1016/j.carbon.2009.09.066.

Zhu X., Yu S., Xu K., Zhang Y., Zhang L., Lou G., Wu Y., Zhu E., Chen H., Shen Z., Bao B. and Fu S., 2018. "Sustainable activated carbons from dead ginkgo leaves for supercapacitor electrode active materials". Chem. Eng. Sci., **181**: 36–45, doi: 10.1016/j.ces.2018.02.004.

Zingare P.A., Dhoble S.J. and Deshmukh A.D., 2022. "Highly stable fish-scale derived lamellar carbon for high performance supercapacitor application". Diam. Relat. Mater., **124**: 108925, doi: 10.1016/j.diamond.2022.108925.